GEOPHYSICAL RESEARCH LETTERS, VOL. 33, L15105, doi:10.1029/2006GL026220, 2006

Tether-induced airglow: Collisionless effects

E. V. Mishin[1] and G. V. Khazanov[2]

Received 14 March 2006; revised 10 May 2006; accepted 22 June 2006; published 4 August 2006.

[1] A specially-designed sounding rocket experiment with a bare, conducting tether was recently suggested to test an idea that tether-produced energetic-electron beams can be used for remote sensing the neutral density in the E region. This letter contains the theoretical analysis of collisionless beam-plasma interactions (BPI) that complement direct impact of the energetic electrons with neutral particles. Collisionless effects are shown to play a significant and even major role in tether-induced aurora (TA). In the F region, BPI lead to appreciable green-line (557.7 nm) emissions at ~200 km. Farther downward, BPI develop inside a local minimum in the plasma density between the E and F regions, the so-called valley. Here a thin layer of a strongly-elevated electron temperature and airglow is predicted. Neutralizing electric currents carried by ionospheric electrons can become unstable in the low-density valley. As a result, developing plasma waves inhibit the currents. In the extreme case, the beam might be locked (a 'virtual cathode'). In addition to optical observations, these effects can also be observed by radio frequency methods. **Citation:** Mishin, E. V., and G. V. Khazanov (2006), Tether-induced airglow: Collisionless effects, *Geophys. Res. Lett.*, *33*, L15105, doi:10.1029/2006GL026220.

1. Introduction

[2] *Martinez-Sanchez and Sanmartin* [1997] (hereafter MSS97) showed that ion bombardment of a bare, conducting tether in the ionosphere and acceleration in the tether potential would produce energetic electron beams. In the mid-latitude F region (magnetic dip angles $\chi \sim 40°-50°$ and the plasma density $n_c \simeq 10^6$ cm^{-3}), the tether of a length 20 km would yield electron fluxes $q_b \simeq 10^{10}$ cm^{-2}s^{-1} and energies $\varepsilon_b \simeq 3$ keV. As in natural aurorae, collisions of the energetic electrons with neutral particles should produce airglow in the E region, i.e., tether-induced aurora (TA). Since the neutral density can be deduced from the auroral volume emission rates [e.g., *Rees*, 1989], MSS97 suggested that tether-produced electron beams can be used for remote sensing the neutral density in the E region.

[3] A specially-designed sounding rocket experiment with a bare, conducting tether of ~1 km length and −3 kV potential was recently suggested to test this idea [*Fujii et al.*, 2005]. To ensure successful observations, all possible interactions of the energetic electrons with the ionosphere should be accounted for. The TA-based method implies that unlike intense electron beams injected from spacecrafts [e.g., *Grandal*, 1982], tether-produced beams are not subject to collisionless beam-plasma interactions (BPI). However, it is established that BPI can play an important role in natural aurorae for similar beam parameters. In particular, this regards to thin layers of enhanced ionization/airglow and elevated electron temperatures in the auroral ionosphere [e.g., *Stenbaek-Nielsen and Hallinan*, 1979; *Wahlund et al.*, 1989; *Mishin and Telegin*, 1989; *Voronkov and Mishin*, 1993; *Schlesier et al.*, 1997].

[4] This letter contains the theoretical analysis of collisionless effects that complement direct impact of the tether-produced energetic electrons with neutral particles. These effects are shown to play a significant and even major role in the tether-induced aurora, leading to the beam's scattering and green-line emissions in the F region. Farther downward, BPI develop in the transition region between the E and F regions, the so-called valley [e.g., *Titheridge*, 2003]. As a result, a thin layer of a strongly elevated electron temperature (T_e) and airglow develops well above the collisional TA, similar to those observed in the auroral ionosphere [*Voronkov and Mishin*, 1993; *Schlesier et al.*, 1997].

[5] The beam current $j_b = e \cdot q_b \simeq 15$ μ A/m^2 must be compensated by ionospheric electrons. In the F region, the ionospheric current velocity $u_c \simeq 10^{10}/n_c$ is well below the current-driven instability threshold [e.g., *Mikhailovskii*, 1974]. However, the plasma density in the valley drops to $\leq 10^3$ cm^{-3} [e.g., *Titheridge*, 2003], yielding u_c of the order of the thermal electron velocity $v_{T0} = \sqrt{2T_{e0}/m}$. As a result, plasma waves can develop and inhibit the currents. In the extreme case, the beam may be locked near the valley 'bottom' analogous to a virtual cathode. A schematic of TA that accounts for collisionless effects is depicted in Figure 1, where r_L is the beam gyroradius and **B** is the geomagnetic field (cf. MSS97). In addition to optical observations, electrostatic plasma waves excited in the course of BPI and elevated electron temperatures can be detected by incoherent scatter radars [e.g., *Schlesier et al.*, 1997].

2. BPI Effects in the F Region

[6] In the proximity of the tether, the pitch-angle distribution of downward-propagating electrons emitted from unit length is $f_\theta = \frac{2n_b}{\pi} \frac{\sin\theta}{\sqrt{\cos^2\chi - \cos^2\theta}}$ at $\chi \leq \theta \leq \frac{\pi}{2}$ (MSS97), where $n_b = q_b/v_b \sim 3$ cm^{-3}, $v_b = \sqrt{2\varepsilon_b/m}$. Note that for upward-propagating electrons $\theta \rightarrow \pi - \theta$. Accelerated electrons follow their gyro-trajectories and quickly ($\Delta t < 1$ ms) form a curtain-like beam: $\Delta y \sim 2r_L = 2v_{b\perp}/\Omega \ll \Delta z \simeq L_t$ and $\Delta x \simeq L_t/\tan\chi$ (the inset in Figure 1). Here $v_{b\perp} = v_b \sin\theta$, $\Omega \simeq 8.2\ 10^6$ s^{-1} is the electron gyrofrequency, the axis $\hat{\mathbf{z}}$ and $\hat{\mathbf{x}}$ coincide with the local vertical and the horizontal geomagnetic component, respectively. Notice that the minimum of the beam dwell time $\tau_\perp \sim 2r_L/V_R$ is of order

[1]Institute for Scientific Research, Boston College, Chestnut Hill, Massachusetts, USA.
[2]NASA Marshall Space Flight Center, Huntsville, Alabama, USA.

0094-8276/06/2006GL026220$05.00

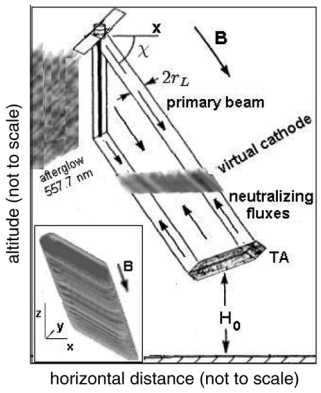

Figure 1. Cartoon depicting the tether-induced airglow with collisionless interactions included. Inset shows some trajectories of electrons emitted from adjacent sites of the tether.

10 ms, provided the payload's speed along the $\hat{\mathbf{y}}$-axis is $V_R \sim$ 1 km/s. As a result of the overlap of trajectories originating from adjacent (vertical) sites of the tether, the distribution function (DF) in the beam's core can be approximated as

$$f_b(v_\parallel, v_\perp) = n_b f_\parallel\left(\frac{|v_\parallel - U_\parallel|}{\Delta U_\parallel}\right)\cdot f_\perp\left(\frac{|v_\perp - U_\perp|}{\Delta U_\perp}\right) \qquad (1)$$

[7] Here $U_\parallel = \langle v_{b\parallel}\rangle = \frac{2\cos\chi}{\pi}\, v_b \approx 0.45\, v_b$ and $U_\perp = \langle v_{b\perp}\rangle = \frac{2}{\pi}E(\cos\chi)\cdot v_b \approx 0.86\, v_b$ are the average parallel and transverse to **B** velocities, $\Delta U_\parallel = \sqrt{\left\langle \left(v_{b\parallel} - U_\parallel\right)^2\right\rangle} \approx 0.3\cos\chi\, v_b \approx 0.22\, v_b$ and $\Delta U_\perp = \sqrt{\left\langle \left(v_{b\perp} - U_\perp\right)^2\right\rangle} \approx 0.1\, v_b$ are their velocity spreads, $\langle\rangle$ stands for averaging over pitch angles, and E(a) is the second order complete elliptic integral; $\chi = 45°$ is assumed for numerical estimates. The exact form of $f_\parallel$ and $f_\perp$ in equation (1) is not important, only the conditions $f_{\parallel,\perp}(|x| \to \infty) \to 0$ and $\int f_\parallel \cdot f_\perp\, d^3v = 1$ are assumed.

[8] Since $U_{\perp,\parallel} > \Delta U_{\perp,\parallel} \gg v_{T0}$, the distribution (1) is close to the so-called "warm" beam in $v_\parallel$ and to the beam of "oscillators" in $v_\perp$, respectively. The latter excites upper hybrid (*uh*) $\omega_{uhr} = \sqrt{\omega_p^2 + \Omega^2}$ and electron Bernstein (*eb*) waves, $\omega_s(k)/\Omega = s + \delta_s(k)$. Here $\omega_p \approx 6\ 10^4\ \sqrt{n_c}\ \mathrm{s}^{-1}$, $s = 1, 2, \ldots$, and $|\delta_s(k)| < 1/2$. The growth rate of short-scale $\sqrt{\varepsilon_{b\perp}/T_{e0}} \gg k_\perp r_L \gg 1$ oscillations with $k_\parallel < k_{\parallel s} \simeq k_\perp\sqrt{\gamma_\perp/\Omega}$ maximizes near the so-called double plasma resonance $\omega_{uhr}(z_s) = \sqrt{\omega_p^2 + \Omega^2}\Big|_{z_s} \to s\cdot\Omega$ [e.g., *Mikhailovskii*, 1974]

$$\gamma_\perp \simeq \frac{1}{2}\Omega\left(\frac{n_b}{n_c}\frac{U_\perp}{\Delta U_\perp}\right)^{1/2} \qquad (2)$$

[9] For $n_b/n_c = 3\ 10^{-6}\ \mathrm{cm}^{-3}$, one gets $\gamma_\perp \simeq 2\ 10^4 \gg \nu_e \sim 10^3\ \mathrm{s}^{-1}$ (the elastic collision frequency of thermal electrons). The plasma density varies with altitude, and the frequency mismatch $|\omega_{uhr}(z) - s\cdot\Omega| \simeq |\Delta z\cdot\frac{d}{dz}\omega_{uhr}| \simeq 2\pi|\Delta z|\cdot 40\ \left[\frac{\mathrm{kHz}}{\mathrm{km}}\right]$ destroys the resonance ($\to 0.1\ \Omega$) at $|\Delta z_s| \simeq 3$ km, provided the density gradient scale-length $L_n = n_c/|\nabla_\parallel n_c| \simeq 50$ km below the F-maximum. In the proximity of the F-maximum one has $|\Delta z_s| \gg 10$ km. Since $\gamma_\perp \cdot \tau_\perp \gg \Lambda \sim 10$ (the Coulomb logarithm), the unstable beam-wave system has time to reach saturation [e.g., *Sagdeev and Galeev*, 1969]. In the saturated state, the wave energy density W_s is of the order of the initial beam transverse energy [e.g., *Aburdgania et al.*, 1978], i.e., $W_s \simeq 0.3 n_b m U_\perp^2 \simeq 10^3\ \mathrm{eV/cm}^3$. Note that the excitation of double-plasma resonances in the F region was observed during injections of weak electron beams from the shuttle [*Gough et al.*, 1995].

[10] The r.m.s. amplitude, $E_s = \sqrt{4\pi W_s} \simeq 2$ V/m, is well beyond the threshold $E_{pd} \simeq 10^{-2}\ \left[\frac{\mathrm{V}}{\mathrm{m}}\right]$ for parametric decay into secondary *uh*/*eb* waves [*Zhou et al.*, 1994]. The waves' rise time, $\sim 2\Lambda(E_{pd}/E_s)\,\nu_e^{-1}$, is much less than $\tau_\perp$ and hence tertiary waves will be generated, etc. The resulting wave energy spectrum consists of a few spectral peaks, each of order $(\Lambda\nu_e/\gamma_\perp)^{1/2}\, E_s$ (well-known weak turbulence "cascading" [e.g., *Sagdeev and Galeev*, 1969]). The r.m.s. amplitude of the total *uh*/*eb* field is $E_\Sigma \simeq 2E_s$.

[11] *Dimant et al.* [1992] and *Grach* [1999] showed that acceleration by *eb*/*uh* waves via cyclotron resonance $v_\parallel = (\omega(k) - s\Omega)/k_\parallel$ is a key source of suprathermal electrons in ionospheric HF heating experiments. Photoelectrons present in the F region during twilight provide many more "seed" electrons for acceleration than are available with a Maxwellian distribution [e.g., *Grach*, 1999]. At $k_\parallel < k_{\parallel s}$ and $\frac{1}{2}mv_\parallel^2 \sim 10$ eV, for acceleration to be efficient the frequency mismatch must be less than 0.1 Ω. This is valid along the whole turbulence layer. The accelerated electron population depends directly on the resonance waves' energy and the acceleration time $\sim\Delta z_s/v_\parallel$. Both the wave energy W_s and the layer's length Δz_s essentially exceed those characteristic of the HF heating. Thus, the values of the density $n_a \simeq (10^{-4} - 10^{-3})\, n_c$ of accelerated electrons with energies up to $\varepsilon_a \simeq 50$ eV, obtained for the HF heating, can be considered as the lower limit.

[12] Atomic oxygen O is the main neutral constituent in the F region above ~200 km. Transitions from the $O(^1S)$ state to $O(^1D)$ yield 557.7-nm (green-line) photons. Collisional quenching of the $O(^1S)$ state in the F region is negligible. Its volume excitation rate is $Q_{1S} = N_O\cdot 4\pi\int_{\varepsilon_{1S}}^{\infty}\sigma_{1S}(\varepsilon)\,\Phi_a(\varepsilon)d\varepsilon \simeq 10^{-9} n_a N_O\ \mathrm{cm}^{-3}\mathrm{s}^{-1}$. Here N_O is the oxygen density, $\Phi_a(\varepsilon) \simeq n_a\sqrt{2\varepsilon_a/m}/(4\pi\varepsilon_a)$ is the differential number flux, $\sigma_{1S} \simeq 310^{-18}\ \mathrm{cm}^2$ at 7–20 eV, and $\varepsilon_{1S} \approx$ 4.2 eV [e.g., *Bernhardt et al.*, 1989]. Figure 2 shows the energy loss of accelerated electrons in eV/km at different altitudes, calculated with *Majeed and Strickland*'s [1997] cross-sections for winter conditions at mid latitudes. Given the acceleration region near 300 km, accelerated electrons propagate downward to $z_a \sim 200$–220 km. For ε_a in the range 10–50 eV and $n_a \sim 10^3\ \mathrm{cm}^{-3}$, the column emission rate at magnetic zenith is estimated as $10^{-6}\int_{z_a}^{z_s} Q_{1S}\, dz\cdot\tau_\perp \simeq 10^{3.5}\,\tau_\perp \simeq 30$ Rayleighs (R) at $\tau_\perp = 10$ ms. Although small, it is well above the sensitivity threshold of contemporary optical imagers of order a few R [e.g., *Pedersen and Carlson*, 2001].

[13] Note that the distribution of upward-propagating electrons is also described by equation (1), where $U_\parallel$ is replaced by $-U_\parallel$. Therefore, their collisionless effects in the F-region are roughly the same as those of downward-propagating electrons. Second, the beam density n_b is

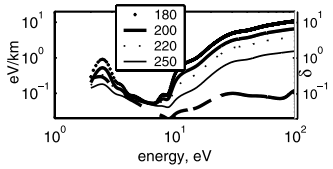

Figure 2. Energy loss of suprathermal electrons at different altitudes (the left axis). The dashed line shows the ratio δ between inelastic and elastic collision frequencies at 250 km.

proportional to the plasma density near the tether $n_c = n_0$ [MSS97]. Thus, the growth rate (2) $\propto \sqrt{n_b/n_0}$ does not change with n_0, while W_s and, most significantly, n_a do. As a result, the intensity of green-line emissions in the weakening F region will decrease, reaching the observational threshold at $n_0 \sim n_* = 10^5$ cm^{-3}.

3. Collisionless Effects in the *E* Region

[14] Since relaxation over transverse velocities does not affect the beam distribution over $v_\parallel$, Langmuir waves with phase velocities $\omega_l/k_\parallel < U_\parallel - \Delta U_\parallel$ can grow with the rate $\gamma_\parallel \simeq \omega_p \frac{\pi n_b}{2n_c}\left(\frac{U_\parallel}{\Delta U_\parallel}\right)^2 \gg \nu_e$. For the waves to develop within the dwell time, $\gamma_\parallel \cdot \tau_\perp$ must exceed Λ. This yields $n_c < n_c^* \simeq 2\ 10^4 n_b^2$ cm^{-3}. For the unstable beam-wave system to reach saturation in inhomogeneous plasmas, it is necessary that the condition $L_n > L_b \simeq \Lambda \frac{U_\parallel}{\omega_p}\frac{n_c}{n_b}$ is fulfilled [*Vedenov and Ryutov*, 1975]. Since $L_b(n_c^*) \sim 300$ km, the warm-beam instability in the F region is inhibited by the plasma inhomogeneity, except for the proximity of the F-maximum if $n_{\max} < n_c^*$.

[15] In the so-called valley below ~200 km the mean plasma density is $n_v \simeq (1\text{–}1.5)\ 10^3$ cm^{-3} [*Titheridge*, 2003], resulting in $L_b(n_v) \simeq 15$ km. The density altitude-profile has at least one minimum near the entry into the valley. Here the beam instability is particularly favored as $\nabla n_c \to 0$ [cf. *Voronkov and Mishin*, 1993]. From the quasilinear theory [e.g., *Vedenov and Ryutov*, 1975] it follows that the wave energy density W in the saturation is $W_{ql} \simeq \frac{2}{15} n_b \varepsilon_{b\parallel} \frac{U_\parallel \Delta U_\parallel}{v_{e0}^2} \simeq 510^5 \frac{\text{eV}}{\text{cm}^3}$ (cf. $n_v T_{e0} \simeq 75 \frac{\text{eV}}{\text{cm}^3}$ at $T_{e0} = 0.05$ eV). In fact, at $W \geq (M/m)^{1/3} n_v T_{e0}$ the aperiodic parametric instability develops, and electrons are heated to $T_e = T_w \simeq W/(2n_v)$ within the time $\tau_p \simeq 10(M/m)^{1/3}\omega_p^{-1}$ due to wave breaking [*De Groot and Katz*, 1973; *Bauer et al.*, 1992]. Here M is the mean ion mass. Since $\gamma_\parallel \tau_p > 1$, the waves continue rising during the nonlinear heating, resulting in $T_w \simeq \frac{\Lambda}{2}(M/m)^{1/3} T_{e0} \simeq 5$ eV within the layer $\Delta z = L_h \simeq \Lambda \frac{\Delta U_\parallel}{\gamma_\parallel}\frac{n_b \varepsilon_{b\parallel}}{n_v T_w} \simeq 0.5$ km.

[16] Along with the heating, appear short-scale (of order the Debye length) density oscillations with the r.m.s. amplitude $\delta n \simeq (m/M)^{1/6} n_c$ [*Volokitin and Mishin*, 1978]. Conversion on the oscillations leads to the Langmuir waves' damping rate $\gamma_{cnv} \simeq (m/M)^{1/3}\omega_p$. At $\gamma_{cnv} > \gamma_\parallel$ the beam instability is inhibited in the heated layer. Besides, the oscillations lead to the beam scattering over pitch-angles [e.g., *Khazanov et al.*, 1993]. Thus, the BPI begins farther upstream, where the whole process repeats again and again. The propagation speed of this 'heating' wave appears to be $u_h \sim L_h/\tau_p \simeq 10^3$ km/s (cf. the 'relaxation wave' in the pure quasilinear BPI theory [*Vedenov and Ryutov*, 1975]). As a result, the heated layer ~10 km near the valley's entry is formed within the dwell time, if the altitude extent of the density minimum Δz_m exceeds 10 km. Otherwise, the layer's thickness is $\sim \Delta z_m$. Note that this scenario holds as long as $\gamma_\parallel(n_b, n_v) \simeq 10^4 \cdot n_b > \max(\Lambda/\tau_\perp, \nu_e)$, requiring $n_b > 0.4$ cm^{-3} or $n_0/n_* > 1.5$. *Voronkov and Mishin* [1993] and *Schlesier et al.* [1997] suggested a similar scenario, except for the nonlinear heating and conversion, to explain thin layers of elevated T_e observed in the valley during auroral precipitation events. Enhanced plasma waves in the valley were observed during a weak keV- electron precipitation [*Kelley and Earle*, 1988].

[17] Up to this point, it is inferred that the beam current is readily neutralized by ionospheric electrons or that their current velocity $u_c = q_b/n_c$ is below the threshold of current-driven instabilities. In the heated T_w-layer, it is the ion acoustic (IA) instability with $u_{th}^{(ia)} \simeq \sqrt{\frac{T_w}{M}}$ [e.g., *Mikhailovskii*, 1974]. In the background ($T_{e0} \sim T_{i0}$) plasma, it is the Buneman instability with $u_{th}^{(B)} \simeq v_{T0} \simeq 10^7$ cm/s. The latter develops if $n_v < q_b/v_{T0} \simeq 10^3$ cm^{-3}, i.e., only near the density minimum, $n_m < 10^3$ cm^{-3}. Because of the Buneman instability, the effective electron collision frequency becomes $\nu_{ef} \simeq \omega_p\sqrt{\frac{m}{M}}$ [e.g., *Galeev and Sagdeev*, 1984], and the downward ($\parallel$ **B**) electric field $E_\parallel \simeq 4\pi\sqrt{\frac{m}{M}} j_b/\omega_p \simeq 0.01\sqrt{10^3/n_m}$ V/m is established. The anomalous Joule heating $Q_{ef} = j_\parallel \cdot E_\parallel$ increases mainly T_e, so that the IA instability develops shortly ($\Delta t \ll \tau_\perp/\Lambda$).

[18] The saturated spectrum of ion acoustic turbulence is subjected to a complex play of various conditions [e.g., *Galeev and Sagdeev*, 1984]. In the case where $u_c \gg u_{th}^{(ia)}$, the ion-acoustic spectrum depends mainly on whether or not a non-Maxwellian tail of energetic ions that absorb the wave energy is formed. In the ionosphere, it is mainly defined by ion-neutral collisions [*Mishin and Fiala*, 1995]. Roughly, at altitudes below ~150 km the tail cannot be created. In this case one has $\nu_{ef} \simeq \frac{10^{-2} T_e}{T_i}\frac{u_c}{v_e}\omega_p$ (Sagdeev's formula). The resulting electric field is $E_\parallel \simeq 0.05 T_e^{1/2}(10^3/n_m)^{3/2}$ V/m, provided $T_i \sim T_{i0}$ due to ion-neutral collisions.

[19] In the T_w-layer, one has $T_e = T_w$. If there are two density minima in the valley [e.g., *Titheridge*, 2003], in the lower one T_e is defined by the condition $Q_{ef} = n_m \nu_e \delta(T_e) T_e$. Here $\nu_e \simeq 210^{-7} N_n \sqrt{T_e}$ and $\delta(T_e)$ is the coefficient of inelastic losses. At $N_n \simeq 510^{10}$ cm^{-3} (at ~150 km) one gets $T_e^{(m)} \sim 6$ eV and $E_\parallel^{(m)} \sim 0.1\ (10^3/n_m)^{5/2}$V/m. At $n_m \simeq 600$ cm^{-3} and $\Delta z_m \sim 10$ km, the potential drop $E_\parallel^{(m)} \cdot \Delta z_m$ exceeds ε_b/e and thus the beam will be locked in this region.

[20] In the weakening ionosphere, the development of the IA instability in the T_w-layer is practically not affected until $n_0 > n_*$. However, the development of the Buneman instability is inhibited, unless $n_m < 10^{-3} n_0$. Finally, electrostatic plasma waves excited in the course of BPI and elevated electron temperatures can be detected by the radar technique [e.g., *Schlesier et al.*, 1997].

4. Conclusion

[21] It is shown that during a sounding rocket experiment with a conducting tether, collisionless effects can play a key role in the interaction of the tether-created, energetic electron beam with the ionosphere. In the F region, BPI will

lead to losses of the beam transverse energy and green-line (557.7 nm) emissions. In the valley between the E and F regions, BPI will result in losses in the parallel beam energy, leading to strong electron heating and airglow. Finally, the development of current-driven instabilities in the low-density valley may inhibit neutralizing currents, thereby locking the beam near the valley 'bottom'.

[22] **Acknowledgments.** We thank the referees for constructive comments. E. V. M. was supported in part by AFRL contract F19628-02-C-0012 with Boston College. G. V. K. was funded in part by the In-Space Propulsion Technology Program of NASA's Science Mission Directorate through the In-Space Propulsion Technology Office at Marshall Space Flight Center under the Technical Task Agreement M-ISP-04-37.

References

Aburdgania, X., A. Kitzenko, and I. Pankratov (1978), The nonlinear stage of charged particle beam interaction with magnetized plasmas, *Sov. J. Plasma Phys.*, *4*, 227.

Bauer, B., A. Wong, V. Decyk, and G. Rosenthal (1992), Experimental observation of super strong electron plasma waves and wave breaking, *Phys. Rev. Lett.*, *68*(25), 3706.

Bernhardt, P., C. Tepley, and L. Duncan (1989), Airglow enhancements associated with plasma cavities formed during ionospheric heating experiments, *J. Geophys. Res.*, *94*, 9071.

De Groot, J., and J. Katz (1973), Anomalous plasma heating induced by a very strong high-frequency electric field, *Phys. Fluids*, *16*, 401.

Dimant, Y., A. Gurevich, and K. Zybin (1992), Acceleration of electrons under the action of intense radio-waves near electron cyclotron harmonics, *J. Atmos. Terr. Phys.*, *54*, 425.

Fujii, H., et al. (2005), A proposed bare-tether experiment on board a sounding rocket, paper presented at 9th Spacecraft Charging Conference, Japan Aerospace Explor. Agency (JAXA), Tsukuba, Japan.

Galeev, A., and R. Sagdeev (1984), Current-driven instabilities and anomalous resistivity of plasmas, in *Basic Plasma Physics*, vol. II, edited by A. Galeev and R. Sudan, p. 271, Elsevier, New York.

Gough, M., M. Oberhard, D. Hardy, W. Burke, L. Gentile, B. McNeil, K. Boundar, D. Thompson, and W. Raitt (1995), Correlator measurements of MHz wave-particle interactions during electron beam operations on STS-46, *J. Geophys. Res.*, *100*, 21,561.

Grach, S. (1999), On kinetic effects in ionospheric F-region modified by powerful radio waves, *Radiophys. Quantum Electron., Engl. Transl.*, *42*, 572.

Grandal, B. (Ed.) (1982), *Artificial Particle Beams in Space Plasma Studies*, Springer, New York.

Kelley, M., and G. Earle (1988), Upper hybrid and Langmuir turbulence in the auroral E region, *J. Geophys. Res.*, *93*, 1993.

Khazanov, G., T. Neubert, G. Gefan, A. Trukhan, and E. Mishin (1993), A kinetic description of electron beam ejection from spacecraft, *Geophys. Res. Lett.*, *20*, 1999.

Majeed, T., and D. Strickland (1997), New survey of electron impact cross sections for photoelectron and auroral electron energy loss calculations, *J. Phys. Chem. Ref. Data*, *26*, 335.

Martinez-Sanchez, M., and J. Sanmartin (1997), Artificial auroral effects from a bare conducting tether, *J. Geophys. Res.*, *102*, 27,257.

Mikhailovskii, A. (1974), *Theory of Plasma Instabilities*, vol. 1, Instabilities of a Homogeneous Plasma, Consultants Bureau, New York.

Mishin, E., and V. Fiala (1995), Radiation of whistlers by the ion-acoustic turbulence in the ionosphere, *J. Geophys. Res.*, *100*, 19,695.

Mishin, E., and V. Telegin (1989), Effects of plasma turbulence on auroras, *Geomagn. Aeron., Engl. Transl.*, *29*, 1.

Pedersen, T., and H. Carlson (2001), First observations of HF heater-produced airglow at the High Frequency Active Auroral Research Program facility: Thermal excitation and spatial structuring, *Radio Sci.*, *36*, 1013.

Rees, M. (1989), *Physics and Chemistry of the Upper Atmosphere*, Cambridge Univ. Press, New York.

Sagdeev, R., and A. Galeev (1969), *Nonlinear Plasma Theory*, Benjamin, White Plains, N.Y.

Schlesier, A., E. Mishin, and K. Schlegel (1997), "Non-collisional" ionization and temperature layers in the auroral E/F1 layer: EISCAT observations, *Geophys. Res. Lett.*, *24*, 1407.

Stenbaek-Nielsen, H., and T. Hallinan (1979), Pulsating aurora: Evidence for non-collisional thermalisation of precipitating electrons, *J. Geophys. Res.*, *84*, 3257.

Titheridge, J. E. (2003), Ionisation below the night F2 layer—A global model, *J. Atmos. Sol. Terr. Phys.*, *65*, 1035.

Vedenov, A., and D. Ryutov (1975), Quasilinear effects in flow instabilities, in *Reviews of Plasma Physics*, vol. 6, p. 3, edited by M. Leontovich, Consultants Bureau, New York.

Volokitin, A., and E. Mishin (1978), Initial stage of the neutralization of a rocket when an electron beam is injected in the ionosphere, *Sov. J. Plasma Phys.*, *4*, 531.

Voronkov, I., and E. Mishin (1993), Quasilinear regime of Langmuir turbulence in the auroral E region of the ionosphere, *Geomagn. Aeron., Engl. Transl.*, *33*, 350.

Wahlund, J., H. Opgenoorth, and P. Rothwell (1989), Observation of thin auroral ionization layers by EISCAT in connection with pulsating aurora, *J. Geophys. Res.*, *94*, 17,223.

Zhou, H., J. Huang, and S. Kuo (1994), Cascading of the upper hybrid/electron Bernstein wave in ionospheric heating experiments, *Phys. Plasmas*, *1*, 3044.

G. V. Khazanov, NASA Marshall Space Flight Center, Huntsville, AL 35812, USA. (george.khazanov@nsstc.nasa.gov)

E. V. Mishin, Institute for Scientific Research, Boston College, 402 St Clements Hall, 140 Commonwealth Avenue, Chestnut Hill, MA 02467-3862, USA. (evgenii.mishin@hanscom.af.mil)